Journal of Building Engineering 90 (2024) 109383

Contents lists available at ScienceDirect

Journal of Building Engineering

journal homepage: www.elsevier.com/locate/jobe

Self-healing of macroscopic cracks in concrete by cellulose fiber carried microbes

Emmanuel Igbokwe [a,b], Samuel Ibekwe [a], Patrick Mensah [a], Ogad Agu [a], Guoqiang Li [a,b,*]

[a] Department of Mechanical Engineering, Southern University, Baton Rouge, LA, 70813, USA
[b] Department of Mechanical & Industrial Engineering, Louisiana State University, Baton Rouge, LA, 70803, USA

ARTICLE INFO

Keywords:
Self-healing concrete
Lysinibaccilus Sphaericus Bacteria
Cellulose fibers
3D-printed polymeric scaffold
Bio-mineralization
Macroscopic cracks
Mechanical properties
Sustainable infrastructure

ABSTRACT

This research introduces a new approach to healing millimeter scale cracks in concrete using Lysinibaccilus Sphaericus Bacteria (*LSB*) encapsulated in cellulose fibers. Cracking in concrete, particularly macroscopic cracking, can cause premature structural failure and reduce its lifespan, which is a critical industry challenge. While bacteria encapsulated in cellulose fibers have been used to heal cement mortar, the studies are limited to heal much narrower cracks. In this study, we integrate *LSB*, known for its strong biocalcification abilities, with the protective environment of cellulose fibers, which are renewable and sustainable, for healing millimeter scale cracks in ordinary cement concrete. To understand the healing process, we firstly used a 3D-printed polymeric scaffold for preliminary observations of calcite precipitation, demonstrating the potential of bacteria-induced calcification in a controlled environment before applying these insights to concrete. We then studied the self-healing of concrete. Through mechanical testing, we identified the optimal concentration of cellulose fiber as 0.45 % by volume of mortar. Approximately 2.38×10^8 bacteria were immobilized in each gram of cellulose fibers. With cellulose fiber encapsulated *LSB*, the test results show up to 25 % increase in compressive strength and split tensile strength. After crack healing, the self-healing concrete still has higher mechanical strength than the undamaged control concrete. Particularly, the self-healing concrete was able to heal cracks up to 2.5 mm wide in fully wet environments and 1.5 mm wide in wet-dry conditions. This research also highlights the resilience of bacteria carried by cellulose fibers against harsh environmental conditions, including high temperatures at 160 °C, ensuring the durability and applicability of the proposed self-healing concrete in diverse climates. Integrating cellulose fibers encapsulated *LSB* into concrete represents a significant breakthrough in addressing the perennial problem of concrete cracking, offering a promising avenue for constructing durable and maintenance-free structures.

1. Introduction

Concrete is dominant in the global construction sector and is prized for its affordability, durability, high compression strength, and high stiffness. Despite these advantages, concrete exhibits low tensile strength and is susceptible to cracks from various sources, like fatigue, extreme temperature, inadvertent loading, and moisture loss [1,2]. These cracks, inevitable during the service life of concrete,

* Corresponding author. Department of Mechanical Engineering, Southern University, Baton Rouge, LA, 70813, USA.
E-mail address: lguoqi1@lsu.edu (G. Li).

https://doi.org/10.1016/j.jobe.2024.109383
Received 19 January 2024; Received in revised form 18 March 2024; Accepted 16 April 2024
Available online 18 April 2024

can compromise structural integrity, leading to issues like moisture infiltration, reinforcement corrosion, and overall material degradation.

The ramifications of catastrophic failures and compromised structural performance are significant both in financial and human terms. The American Association of State Highway and Transportation Officials (AASHTO) estimated that, when the costs for mandatory yearly inspections and traffic restrictions are not included, the national cost of repairing substandard bridges exceeds $140 billion [3]. The immediate repair of such scenarios is hindered by financial constraints, necessitating long-term solutions through transformative technologies to substantially reduce infrastructure evaluation, assessment, maintenance, and repair expenses. Various repair methods have been employed to address concrete cracks, such as external bonding of fiber-reinforced polymer (FRP) sheets in reinforced concrete beams and columns [4,5], or applying an engineered cementitious composite (ECC) layer and steel plate [6]. While successful, these methods require intensive preparation and may necessitate traffic interruptions or payload removal in buildings. Thus, there is a growing interest in crack self-healing solutions.

Self-healing concrete offers a proactive substitute for reactive crack countermeasures. Materials exhibiting self-healing properties have proven effective in reducing permeability and restoring strength and stiffness. An autonomous capsule-based mechanism in polymer-modified concrete, akin to microencapsulation in polymer self-healing, has been explored [7–9]. This system uses one-part epoxy drops with a liquid core and a hardened shell as a container for the healing agent. After being released into the concrete matrix, the epoxy hardens by reacting with hardener, which assists in repairing cracks and restoring its mechanical properties. Applying microencapsulation techniques to various cement-like substances has led to introducing microcapsules with unique shell materials and healing agents [7].

In recent years, there has been a surge in using bacteria for self-healing purposes [10–17]. The differences among these studies persist in the use of different bacteria and different bacteria carriers. One approach is to embed nutrients and bacteria within sphere-shaped or cylinder-like micro- or macro-capsules. As propagating fracture encounters these capsules, the capsule ruptures and releases bacteria and vitamins that initiate precipitation for crack healing. For example, Wang et al. [10–12] used several bacteria encapsulated in various containers for healing cement mortars. The maximum crack width healed was up to 0.5 mm. Using encapsulation method, challenges arise due to the low capsule concentration in the concrete matrix, especially for spherical capsules with limited opportunities to interact with cracks. Cylindrical capsules, while having a larger bonding area, face challenges with reduced vitamin release because of the suction impact on the closed end [18,19]. Typically, bulk emulsifying polymerization strategies are used for producing microcapsules, which raises questions regarding the dimensions of the capsules and their adhesive capacity with the concrete mix design [20]. The method demands sophisticated equipment and intricate processes. Another challenge is that, like polymer self-healing, once the healing agent and nutrient are released from the capsules, they result in new pores or new defects [21, 22]. Therefore, other bacteria carriers are further explored.

An alternative approach involves the adsorption method, where microbes and minerals are embedded in a permeable fabric with intense pore size, saturated with bacterial suspension. This porous fabric provides support for bacteria growth, as well as oxygen and water retention crucial for microbiologically induced calcite precipitation. Numerous carriers have been used, including diatomaceous earth, polyurethane, ceramics, etc. [23–28]. However, the complexity in the immobilization strategies and high cost have restricted their widespread use in the building sector.

In recent years, various types of fibers have been used as a bacteria carrier in healing cracks in mortar or concrete. The advantage of using fibers as carriers is that fibers not only provide a protective environment for bacteria, but also serve as a reinforcement to increase concrete strength and reduce crack opening. Su et al. [29] used polypropylene (PP) fiber as a bacteria carrier and shows higher healing efficiency. However, none of them have focused on healing wide-opened, millimeter scale cracks in concrete. Singh and Gupta [30] investigated the potential of cellulose fiber as a bacteria carrier in mortar and quantified self-healing through Ultrasonic Pulse Velocity (UPV). They prepared two types of bacterial mortar using Bacillus subtilis strain 168 and added nutrients to either the mortar mix or the curing water. The effectiveness of crack healing was evaluated using image analysis and UPV tests. The study showed that cellulose fibers, acting as bacteria carriers, could enhance self-healing, although it resulted in a decrease in compressive strength and insufficient physical self-healing. The maximum theoretical crack width was 0.52 mm. In another work, Singh, and Gupta [31] studied the feasibility of alkali-treated micro cellulose fiber as a novel bacteria-carrier for self-healing mortar. The research shows that self-healing mortar using cellulose fiber as a bacteria-carrier results in maximum self-healing as compared to other mixes, 8.23 % more than control samples. However, the studies focused on self-healing of mortars and the maximum crack width of 0.7 mm.

This research focuses on using *lysinibaccilus Sphaericus Bacteria (LSB)* encapsulated within cellulose fibers to target the autonomous healing of millimeter scale cracks in concrete. We choose *LSB* due to its robust biocalcification capabilities, which, combined with the protective and supportive environment provided by cellulose fibers, presents a novel methodology for self-healing at an unprecedented scale. We choose cellulose fibers because they offer distinct advantages, such as being biodegradable and having superior water retention capabilities. These fibers create a conducive environment for bacterial growth which leads to sustained crack-healing activity. Unlike alkali-activated carriers and expanding Perlite, cellulose fibers reduce bacterial leakage and maintain a consistent presence of healing agents within the concrete matrix. This highlights the potential of cellulose fibers as an eco-friendly and efficient solution for self-healing concrete. Unlike earlier studies that focused on microcrack healing in cement mortar or used synthetic carriers, our approach capitalizes on the inherent properties of cellulose fibers to reinforce the mechanical properties of concrete and create a conducive environment for bacterial-induced calcite precipitation, which is essential for the healing of macroscopic cracks. Our experimental design covers a broader spectrum of crack sizes, incorporating more rigorous testing methods not only to assess the healing efficiency but also to evaluate the impact on the mechanical properties and characterization of concrete.

To validate the efficacy of our proposed system, we conducted an initial investigation using calcite precipitation on a 3D printed polymer scaffold. Although the environmental conditions of concrete and scaffold vary, this preliminary study was instrumental in

comprehending the potential of our microbial and cellulose fiber approach. Subsequent experiments were then designed to ensure successful translation of the bio-mineralization process, bridging the gap between controlled laboratory settings and actual concrete applications.

By harnessing the latest advancements in microbial loading technologies and prioritizing the sustainability and efficiency of cellulose fibers as bacteria carriers, this research presents a comprehensive solution to a critical challenge in civil engineering. The novelty of our work lies in its approach to millimeter scale crack healing in concrete, setting a new standard for future research in self-healing concrete technologies geared toward achieving sustainable and resilient infrastructure.

2. Experimental

2.1. Materials

2.1.1. Cement

Ordinary Portland Cement (OPC) Type I GU, which satisfies ASTM C150 specifications for Type I cement, was used to create concrete and mortar samples. The following chemical compositions make up Type I OPC: (a) 40–65 % for tricalcium silicate (C3S); (b) 20–35 % for dicalcium silicate (C2S); (c) 8–12 % for tricalcium aluminate (C3A); (d) 8–12 % for tetra-calcium alumino-ferrite (C4AF); and (e) 5 % for gypsum added during the grinding process [32].

2.1.2. Aggregate

Aggregates, which include coarse and fine, are essential to constructing concrete and other building materials. These granular substances form a robust and enduring concrete matrix when mixed with cement, water, and occasionally additional additives. This investigation employed gravel comprising a blend of crushed stone and natural sand sourced from riverbeds. The particles exhibited the characteristics of being well-graded and rounded. The relative dry densities were measured as 2.69 and 2.65 g/cm^3 for coarse and fine aggregates, respectively. These values were correspondingly accompanied by absorption ratios of 0.70 % and 0.80 %. The largest sizes for the fine and coarse aggregates were 4.50 mm and 10.50 mm, respectively. Table 1 gives specific details regarding the mix design proportions for the concrete.

2.1.3. Cellulose fiber

For this research, the fibers were provided by Solomon Colors, Inc. The manufacturer describes the Ultra-Fiber as a cellulose-based microfiber resistant to alkali that is utilized with better bonding and hydration, crack management, and better reinforcement. The Solomon Inc. Ultra Fiber 500 has a length of 2.1 mm and a diameter of 18 μm. Cellulose fibrils, composed of chains of glucose molecules held together by hydrogen bonds, make up each filament of this cellulose fiber. It exhibits an 80 % water absorption rate, 1.1 g/cm^3 density, and 900 MPa tensile strength compared to 480 MPa for polypropylene. It is more affordable than synthetic fibers and steel fibers because each pound contains 77 million fibers [33]. Since these fibers are produced using naturally occurring renewable resources, they assist in achieving environmental sustainability. Fig. 1 shows the cellulose fiber platelet.

2.1.4. Lysinibaccilus Sphaericus Bacteria (LSB)

The rod-shaped, gram-positive *Lysinibaccilus Sphaericus Bacteria (LSB)* are fully aerobic bacteria. These bacteria form pores and may be dormant for several years. Soil, leaf surfaces, and aquatic habitats can all contain the *LSB*. This variety displays robust enzyme urease action, persistent synthesis of packed limestone minerals ($CaCO_3$), and adverse zeta possibility, all tolerating a temperature as high as 56 °C. This study used the Southern University microbiology lab to cultivate and grow the *LSB* strain ATCC4252. Fig. 2 displays the *LSB* plate colony and SEM picture.

2.1.5. Lattice polymer scaffold

To visualize and understand the calcification brought about by *LSB*, a polymeric scaffold was 3D printed. The 3D polymeric scaffold was designed with the aid of CAD software. The unit cell size of the polymer scaffold is 1.5 mm, and its dimensions are 13.5 × 13.5 × 13.5 mm. Polylactic acid (PLA) was used in the 3D printing of the polymeric scaffold. PLA is a biodegradable and bioactive thermoplastic made primarily from sugarcane or corn starch. It is recognized for having eco-friendly qualities and is a member of the polyester family. PLA is frequently used in medical implants, packaging, disposable dinnerware, and 3D printing. Because of its biodegradability, composability, and reduced environmental impact during production, it has become more and more well-liked as a sustainable substitute for conventional plastics. Because of its good gloss, transparency, and stiffness, PLA can be used in various consumer and industrial applications. Fig. S1 displays the schematic CAD diagram of the 3D polymer scaffold in the Supplementary

Table 1
Mix proportions for the concrete.

Material	Quantities	Units
Cement	320	kg/m^3
Aggregate	750	kg/m^3
Sand	400	kg/m^3
Water	120	kg/m^3
Cellulose Fiber Volume Fraction	0 and 0.45	%
LSB Medium: 2.8 × 10^8 Bacteria/ml	2.38 × 10^8	bacteria/g of cellulose fibers

Fig. 1. Cellulose Fiber Platelet. (Left) 2.1 mm long cellulose fiber platelet and (Right) SEM image of cellulose fiber platelet.

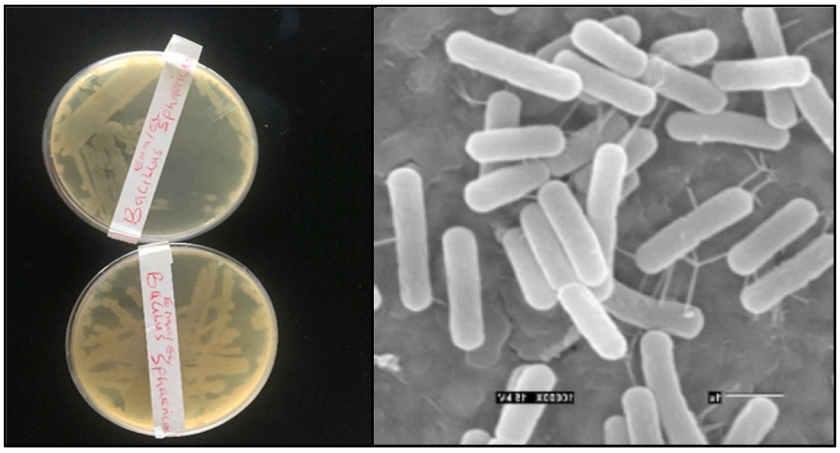

Fig. 2. (Left) the *LSB* colony forming units, and (Right) the SEM Image.

Materials.

2.1.6. Chemicals

A range of chemicals was used in the study to provide nutrients and calcium sources while also promoting bacterial growth and biomineralization. All the chemicals utilized in this research, such as Yeast extract, BatoTM Peptone, calcium chloride anhydrous, calcium nitrate, sodium bicarbonate, urea broth, and ethanol, were purchased from Sigma-Aldrich. To promote microbial activity, the investigation utilized yeast extract as the growth medium, urea as the nitrogen source, and calcium nitrate as the calcium source.

2.2. Experiments

2.2.1. LSB culturing/inoculation procedure and absorption of bacteria in cellulose fiber

The *LSB* bacterial culturing was conducted in nutrient broth, which contained 4.3 g/L of sodium chloride, 2.5 g/L of yeast extract, and 6 g/L of peptone, constituting the solution composition used for *LSB* bacterial culture growth. A magnetic stirring plate was used to stir the mineralization for 10 min at 1400 rpm. The top of the conical flask was completely wrapped in aluminum foil, and the cap was only loosely fastened. Following a 45-min autoclave at 121 °C and 0.14 MPa, the sample was left to cool for a full day at 25 °C temperature. A sterile pipette tip was used to drop one colony from the *LSB* dish into the nutrient broth containing a bio-mineralization solution for inoculation. After inoculation, the solution was placed in an incubator shaken for 48 h at 37 °C and 50 rpm with a loose foil cover. The bacteria growth was determined by a hazy, cloudy substance in the solution that resembled a turbid, yellowish media. The serial dilution method was utilized to adjust the necessary bacterial concentration of 2×10^8 bacteria/ml.

To determine the concentration of Bacteria/ml for *Lysinibaccilus Sphaericus Bacteria (LSB)* serial dilution and colony counting methodologies were used. Firstly, an *LSB* culture was grown in a nutrient-rich broth until it reached an optimal level of bacterial proliferation. Then, serial dilutions ranging from 10^{-1} to 10^{-10} were prepared using sterile Phosphate-Buffered Saline (PBS) as the diluent to preserve bacterial viability during the process. We plated 0.01 ml aliquot onto nutrient agar plates, selecting this dilution level based on preliminary observations. This dilution level yielded approximately 25 single-forming colonies in the plate with a dilution factor of 10^{-5} after incubating at 37 °C for 48 h, which aligns with our target concentration. After the maximum visible

forming colonies were counted, the concentration of the original *LSB* culture was calculated using the formula:

$$\text{Bacteria Concentration} = \text{Total forming colony} / (\text{Volume plated} \times \text{dilution factor})$$

$$\text{Bacteria Concentration} = \frac{25}{0.01\text{ml} \times 10^{-5}} = 2.5 \times 10^{8} \text{Bacteria} \Big/ \text{ml}.$$

The process was meticulously followed according to the guidelines outlined in the American Society for Microbiology's manual for general bacteriological procedures [26]. The bacteria spore solution was preserved in the refrigerator for a longer period using glycerol stock. The inoculation and culturing procedure is depicted in Fig. S2.

In this study, upon adjusting the weight of cellulose fibers to 300 g and considering their 85 % absorption capacity by weight, we aimed to determine the total bacteria immobilized into the cellulose fiber for application in self-healing concrete and Polymer scaffold. Utilizing a bacterial concentration of 2.8×10^8 bacteria per ml, the fibers absorbed 255 ml of this bacterial solution. Consequently, this immobilized approximately 7.14×10^{10} bacteria, or 2.38×10^8 bacteria/g of cellulose fibers, significantly enhancing the potential for efficient crack healing within the concrete matrix. This calculation is foundational to our approach, ensuring a high-density bacterial presence crucial for activating and sustaining the self-healing processes.

2.2.2. Healing procedures in 3D printed polymeric scaffold

This research explored a novel approach leveraging the synergistic properties of cellulose fiber-carrying bacteria to achieve healing capabilities in 3D printed polymeric scaffolds and concrete. To verify whether bacteria could self-heal concrete, the team first applied calcite to a 3D printed polymer scaffold to observe the healing potential.

Our study uses a 3D polymer scaffold coated with calcite to explore the potential of bacteria-induced calcification for concrete self-healing. We acknowledged the significant differences between the scaffold and concrete and utilized the scaffold as a simple model to observe bacterial activity in a controlled environment. This was crucial before applying the findings to the more complex concrete environment. To ensure the survival and effectiveness of bacterial strains in the alkaline conditions of concrete, we adapted the bacterial encapsulation technique and used resilient bacterial strains. We recognize that laboratory results must be translated into practical applications for self-healing concrete. Therefore, our approach aims to bridge the gap between experimental models and real-world structural materials.

Using PLA, a polymeric scaffold with platelet dimensions 13.5 × 13.5 × 13.5 mm was 3D printed at the Southern University CAD Lab. After that, pure ethanol was used to wash the 3D-printed polymer scaffold and dried at 60 °C. A liter of distilled water was used to dissolve calcium chloride 30 g/L, ammonia chloride 12 g/L, nutrition broth 4 g/L, sodium bicarbonate 2 g/L, and urea broth 25 g/L to create the bio-mineralization medium. The mixture was autoclaved for 45 min at 0.1 MPa and 120 °C. Bio-mineralization medium was placed at room temperature (25 °C) after autoclaving; for samples with direct embedding of *LSB*, a 250 ml conical flask filled with *LSB* solution was immersed in dried 3D-printed polymer scaffolds for 24 h at 30 °C. The intention is to guarantee a significant *LSB* bacterial solution surrounding the polymeric scaffold. The scaffolds were then placed in an incubator at 30 °C and immersed in 250 ml bio-mineralization medium. The bio-mineralization medium was changed daily until all the available space of the scaffolds was occupied with calcium carbonate to promote mineral growth. The process known as "bio-mineralization" occurs when bacteria and other living materials help to control the formation of minerals inside biological structures. Bio-mineralization, as used in the context of bacteria-mediated self-healing, describes the capacity of some bacteria to cause the precipitation or deposition of minerals, such as calcium carbonate, as a byproduct of their metabolic processes. This study shows the possibility of utilizing this process to promote materials, such as polymers, to heal themselves. Additionally, 150 g of cellulose fiber was used as a bacteria carrier for polymeric scaffold healing samples. The fiber was immersed in a 1000 ml conical flask containing 500 ml *LSB* solution for 24 h. Following a 24-h period, the bacteria residing in cellulose fiber and polymeric scaffold samples were immersed in a 200 ml bionic mineralization. The samples were placed in a 30 °C incubator and examined every five days to assess the degree of crack closure. Fig. S3 shows the experimental procedure for healing a 3D polymer scaffold. After bacteria mineral encapsulation, bacteria carried by cellulose fibers were dried at 60 °C for 24 h to examine the impact of temperature on the bacteria. After that, the samples were annealed at various temperatures: 60, 100, 120, and 160 °C, respectively, before being brought to the SEM lab to assess the impact of the oven heating. This experimental finding was observed via a decrease in the sizes of bacteria spores. The steps involved in testing the temperature effect are depicted in Fig. S4.

2.2.3. SEM analysis of calcite precipitation around polymeric scaffold and cellulose fiber

Phenom scanning electron microscopy (SEM) inspected the polymer scaffold and calcified cellulose fiber. This investigation aimed to determine if the surface of the fiber bacteria carrier contained calcite, which could help fill the gaps in the polymeric scaffold. Samples of bacteria carriers made of cellulose fiber and polymeric scaffold were annealed and collected in various times to monitor the development of crystallization. The fiber and polymeric scaffold surfaces were analyzed using SEM with an accelerating voltage of 5–15 KV at magnifications ranging from 100 μm to 200 μm. The experimental samples were installed inside the SEM chamber using sample holders and stubs. Fig. S5 shows the procedure of using SEM to observe the structures.

2.2.4. 3D printed polymer scaffold mechanical testing

3D printed polymeric specimens were brought to the MTS lab to determine how calcification affects the strength of materials. The purpose was to analyze the mechanical properties of the (1) control scaffold (without bacteria), (2) with bacteria but without cellulose fiber carrier, and (3) with bacteria carried by cellulose fiber within the 3D printed polymer scaffold. As per IS 516–1959, the test specimens were loaded into a 150 KN universal MTS machine, and the loading rate was adjusted to 1.5 MPa/min until fracture

occurred. Fig. S6 shows the mechanical testing of a 3D polymer scaffold.

2.2.5. Mix design of different concrete specimen

For this study, four sets of concrete cylinders were prepared. The first concrete was the control concrete, denoted as CCxx, which contained only concrete without bacteria or cellulose fibers. The second concrete group was a concrete cylinder with cellulose fibers denoted as FCxx, which accounted for 0.45 % of the mortar volume fraction. The third group was concrete containing bacteria directly incorporated into it without using cellulose fibers, denoted as BCxx. Lastly, the fourth group was concrete, denoted as FBCxx, which contained bacteria carried by cellulose fibers at 0.45 % volume fraction. The four sets of concrete cylinders are summarized in Table 2.

A suitable design mix was created for M25-grade concrete by ASTM C192. The mix comprised a calculated proportion of cement, sand, aggregate, and water, with quantities set at 320 kg/m^3, 400 kg/m^3, 750 kg/m^3, and 120 kg/m^3, respectively. This composition yielded specific ratios crucial for the concrete's performance: a cement-to-sand ratio of 0.8, indicating a slightly higher volume of sand to cement; a water-to-cement ratio of 0.375, selected to ensure optimal hydration without compromising the mix's strength; a sand to the aggregate ratio of approximately 0.53, balancing the fine and coarse components for structural integrity; and a cement to the aggregate ratio of about 0.43, ensuring the cementitious matrix adequately binds the aggregate particles. Every concrete cast was made using a 100 mm by 200 mm cylinder mold lubricated before casting to facilitate sample demolding. Employing an air compressor, the specimens were extracted from the cylinder mold and allowed to cure in water at 25±1 °C until the scheduled test date. The assessment was conducted at 7, 14, and 28 days of age. To determine the cellulose fiber-to-mortar mix design ratio, cellulose fibers of 0 %–0.70 % volume fractions of mortar were investigated via compression testing. The results showed that 0.45 % cellulose fiber achieved the optimum mechanical strength and was adopted in FCxx and FBCxx concrete castings.

In addition to the control concrete without bacteria and cellulose fibers, several concrete specimens were prepared with the same mix design and specimen dimensions FCxx and cellulose fiber at 0.45 % of the mortar volume. In BCxx concrete, the concentration of 2.9 % bacteria (1.04×10^7 bacteria/cm^3 of cement mortar) was combined with 3.5 % calcium nitrate,1 % yeast extract, and 3.5 % urea broth by mortar mass for every concrete cylinder. In FBCxx, cellulose fibers carrying *LSB* bacteria were used. During the concrete casting process, each concrete cylinder in FBCxx received the same number of bacteria as BCxx but carried by 0.45 % cellulose fiber, 3.5 % calcium nitrate, 3.6 % urea broth, and 1 % yeast extract by volume of mortar.

2.2.6. Concrete strength testing

According to IS 516–1959 standard, the mechanical properties of concrete were tested at 7, 14, and 28 days of age, respectively. The cylindrical specimen, measuring 200 mm long and 100 mm in diameter, was subjected to split tensile and compressive tests to evaluate its tensile strength and compressive strength. The test procedures were performed using the heavy-duty 1555 kN Touch 350 Series ELE testing machine.

2.2.7. Concrete water absorption testing

The water absorption test was performed on four types of cylindrical samples using a 100 × 200 mm cylinder mold. Three-cylinder specimens from each type underwent testing in compliance with the ASTM C67-07 standard. Before the test, every cylinder specimen was cleaned and examined for any loose chips and debris. The concrete samples were cured for 28 days and annealed for 24 h at 115 °C in a ventilated oven. The specimens were weighed after they had cooled to room temperature. After that, the dried samples were completely immersed in water from the pipes for a full day at a temperature of 25 ± 1 °C. They were removed, then cleaned with moist fabric, and remeasured.

2.2.8. Acid immersion test

A study was conducted to understand the impact of acid on concrete and calcification. The study used an acid immersion test, following the ASTM C 666–1997 standard. The four types of concrete specimens were submerged in solutions containing 6 % sulfuric acid to test their durability. The percentage of concrete weight and strength loss were calculated and recorded. Weight loss = $[(W_i - W_r)/W_i] \times 100$ %, where W_i depicts the weight before immersion, and W_r represents the weight after immersion. Similarly, Strength loss = $[(S_i - S_r)/S_i] \times 100$ %, where S_i depicts the initial compression strength, and S_r represents the final compression strength after immersion. The percentages of decreased weight and decreased strength were examined after being submerged in H_2SO_4 for 7,14, 28, and 45 days.

2.2.9. Effect of temperature on concrete

Following ASTM C293-16 guidelines, the four types of concrete specimens were put inside a temperature bench oven at 426 °C. The timing was set for 30, 60, 90, 120, and 150 min, respectively. The specimens were cooled to 25 °C after the heating process. The residual compression strength and mass were measured. The purpose of conducting the "Effect of Temperature on Concrete Strength" test is multifaceted and crucial for the comprehensive evaluation of our self-healing concrete. This test aims to ensure the thermal

Table 2
The four types of concrete cylinders.

Specimen	Concrete	Bacteria	Cellulose fiber
CCxx	Yes	No	No
FCxx	Yes	No	Yes
BCxx	Yes	Yes	No
FBCxx	Yes	Yes	Yes

stability of the concrete, which is vital for maintaining consistent mechanical properties across various temperature ranges, directly impacting the material's durability and applicability in different climates. Additionally, understanding how temperature influences the biological activity of the encapsulated bacteria is essential for optimizing the conditions under which the self-healing mechanism operates most effectively. By assessing the material's performance under thermal stress, we can better predict the long-term durability and maintenance needs of infrastructure utilizing self-healing concrete, ensuring structural integrity and safety of such constructions in diverse environmental conditions. Furthermore, insights from this test inform design and application decisions, allowing for the strategic use of self-healing concrete in scenarios where its unique properties can be fully leveraged despite temperature variations. Overall, this section of our study is integral to demonstrating robustness, efficiency, and broad applicability of our innovative concrete solutions.

2.2.10. Procedures for concrete fracture and self-healing

Specimens of concrete from BCxx and FBCxx were subjected to cracking using an MTS machine with a capacity of 150 KN after 28 days of curing. The loading speed was 2.0 MPa/min. The load was gradually applied until a crack appeared, and the fracture was measured with a caliper. The crack measurements ranged between 0.5 mm and 2.5 mm. The fractured specimens were then treated with the fully saturated technique and the wet and dry technique. These methods evaluate the effectiveness of *Lysinibaccilus Sphaericus bacteria (LSB)* in healing cracks. In the wet and dry healing technique, the samples were submerged in water for 24 h and then allowed to stay in the air for 24 h at room temperature; the procedure was repeated until self-healing occurred on a cracked concrete surface after about 25–30 days. Alternatively, the specimens with fully saturated techniques were continuously submerged in water for 25–30 days until the concrete was fully healed.

2.2.11. Structural morphology and crystal formation of concrete

The Phenom SEM was used to investigate the size and shape of precipitated particles. We collected concrete particles from crack locations in BCxx and FBCxx. The specimen was grinded with a sandpaper and pestle until it became powdery and was subjected to X-ray diffraction analysis. The samples were collected at different intervals for examination. The Mini Flex X-ray Diffraction Machine was used for the Study. Cylindrical self-healed samples (4 mm in diameter) from BCxx and FBCxx were also sliced and sent to the SEM lab to determine structural morphology. The samples from BCxx and FBCxx (as shown in Table 2) were placed into the phenom SEM chamber using a sample holder. The specimens were thoroughly cleaned to ensure that the images were not affected.

2.2.12. Compression and split tensile strength testing after concrete self-healing

Compression and split tensile strength after healing were performed again to evaluate the recovery of tensile and compressive strength in self-healing concrete specimens after crack healing, like previous procedures for split tensile and compression tests. Fig. S7 shows the samples under compression and split tensile tests.

3. Results and discussions

3.1. SEM and mechanical analysis for 3D printed polymeric scaffold

The following details are crucial to remember: the addition of bacteria to the nucleation site caused calcification, as shown in Figs. S8 and S9. It took 17 days for the calcification to fill the void in the polymer scaffold. The sequential 3D printed polymer scaffold healing using *LSB* is seen from the SEM images. Day 2 saw no healing, but Days 5 and 10 saw the scaffold begin healing. The scaffold sample had been filled with calcium carbonate on Day 17. Adding cellulose fiber and bacteria enhanced the compressive strength of the polymeric scaffold, as demonstrated by Fig. 3. The samples with the highest compressive strength were FBCxx samples that contained bacteria transported by cellulose fibers. The research indicates that bacteria can help polymer scaffolds heal themselves. In this work,

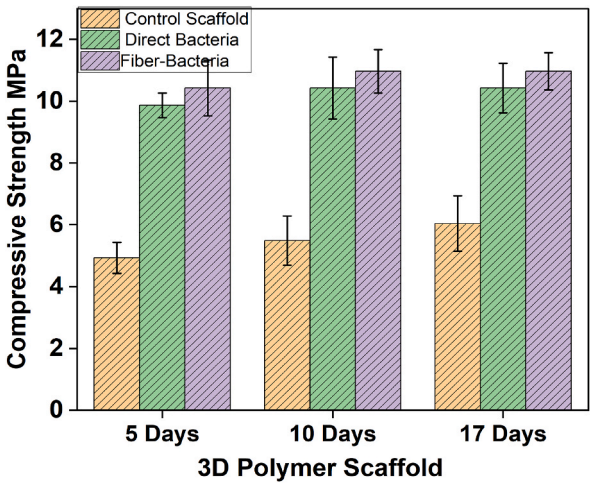

Fig. 3. Compressive strength of 3D printed polymeric scaffold with three types of samples.

the structured β-chitin matrix was replicated by utilizing a 3D-printed polymeric scaffold, with bacteria adherence on the polymeric surface acting as sites for nucleation. The microbial enzyme urease facilitated the crystallization of $CaCO_3$, which surrounded the polymeric scaffold surface.

Bio-mineralized composites with predefined microstructures were produced due to mineral development guided by small pore sizes within the scaffold. In addition to having outstanding specific strength and crack resistance comparable to natural composites, bio-mineralization materials are resistant to high temperatures and harsh conditions. These 3D-printed polymeric scaffolds with fiber carried bacteria not only aid in the understanding and visualization of the calcification procedure but may also find use in industries that demand high-performance structures, such as polymer bridges, vehicle sets, and aircraft boards. The materials are good for body or vehicle armor in defense-related uses because they are light in weight. The chemical reaction is shown below.

$$CO(NH_2)_2 + 2H_20 + Ca^{2+} \xrightarrow{\text{Enzyme}} 2NH_4^+ + CaCO_3$$

3.2. Temperature impact on bacteria carried by cellulose fiber

The SEM images in Fig. 4 demonstrate that bacteria nutrients can withstand hostile environments when cellulose fiber is used as a bacteria carrier at 160 °C. When compared to direct pouring into concrete, which stands around 56 °C [30], the encapsulation of *LSB* in cellulose fiber showed superior temperature resistance. The SEM images presented in this study are integral to understanding the interaction between the bacteria and cellulose fibers, especially following exposure to high temperatures. While SEM images primarily provide morphological evidence, they are critical in illustrating that the bacteria remain physically intact and well-distributed within the cellulose matrix even after thermal stress. This observation is foundational to our hypothesis that cellulose fibers offer a protective environment against high-temperature conditions, thereby preserving the structural integrity of the bacteria. The images indicate that the encapsulation method effectively maintains the bacteria's physical state, a prerequisite for their functional survival and activity. We acknowledge that further quantitative assessments are necessary to prove viability and function post-exposure. However, the SEM results are a promising initial step, suggesting that our encapsulation strategy safeguards the bacteria against thermal degradation, an essential factor for the practical application of self-healing concrete in various environmental conditions.

3.3. Effect of cellulose fiber volume fraction on concrete compressive strength

According to Fig. 5, the findings indicate that adding a volume fraction of 0.45 % cellulose fiber resulted in a 6.5 % increase in the compressive strength of concrete compared to control concrete. The study also suggests that any concentration exceeding 0.45 % of cellulose fiber may lead to decreased strength of the concrete. Therefore, to enhance the compressive strength of the concrete and, at the same time, shield bacteria from being crushed, it is necessary to use a volume fraction of 0.45 % cellulose fiber with respect to mortar.

3.4. Mechanical properties of the four types of concrete

Because the optimal cellulose fiber was determined to be 0.45 % by volume of cement mortar, concrete samples containing bacteria carried by 0.45 % cellulose fibers were examined. Fig. 6 demonstrated that in FBCxx concrete, the split tensile strength was 2.2 MPa, 2.7 MPa, and 3.3 MPa, respectively, and increased by 29.4 %, 35 %, and 32 % when compared to the control concrete (CCxx), which had a split tensile strength of 1.7 MPa, 2.0 MPa, and 2.5 MPa, respectively, on days 7, 14, and 28. From the test results FBCxx concrete produced the most favorable results. The compressive strength of the FBCxx concrete samples was 22.0 MPa, 31.0 MPa, and 38.0 MPa, respectively, which increased by 37.5 %, 34.8 %, and 35.7 % above the CCxx concrete on days 7, 14, and 28, respectively. Therefore, the FBCxx concrete in Table 2 indeed demonstrates the benefit of adding bacteria carried by cellulose fiber in enhancing the strength of conventional concrete.

3.5. Effect of acid on concrete strength

From Fig. 7a&b, after adding 6 % Sulfuric acid in water-submerged concrete samples for 7, 14, 28, and 45 days, CCxx concrete decreased by 14.2 %, 12 %, 14.6 %, and 16.3 % of its compressive strength and 0.23 %, 0.43 %, 1.2 %, and 2.16 % of its weight, in comparison to FBCxx concrete. Compared to the control concrete, the findings demonstrated that concrete containing bacteria

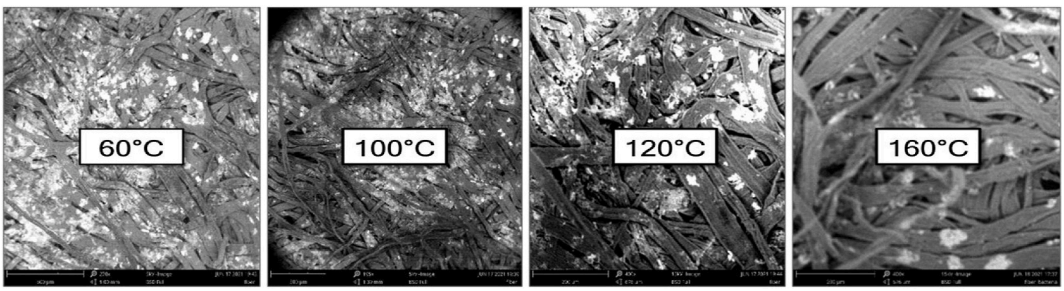

Fig. 4. Temperature impact on cellulose fiber carried bacteria.

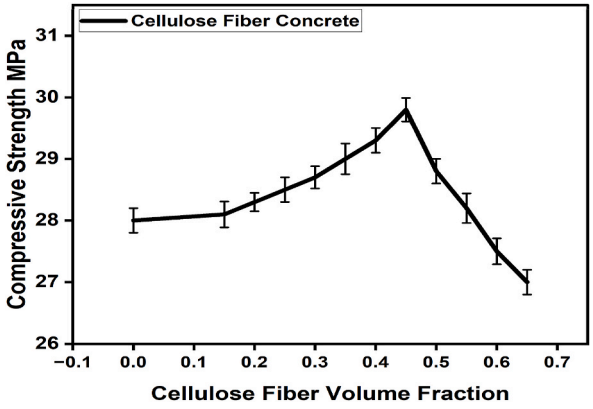

Fig. 5. Effect of cellulose fiber loading on concrete compressive strength.

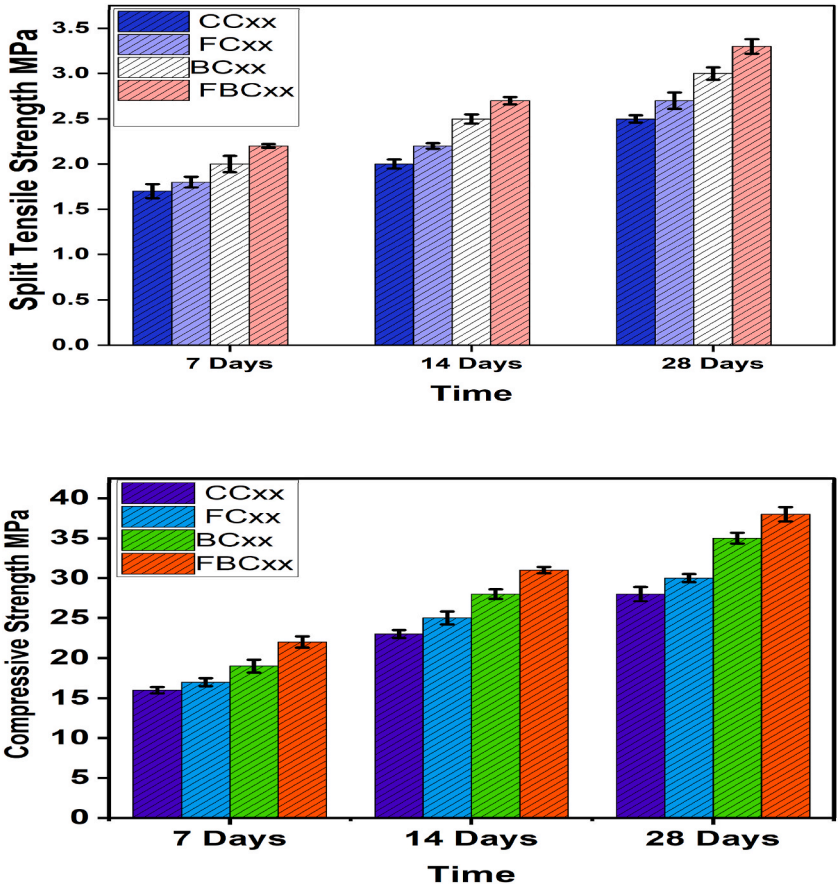

Fig. 6. Mechanical properties of the four types of concrete.

transported by cellulose fibers could survive under precipitated water containing sulfuric acid. The study emphasizes how acid immersion reduces the strength of traditional concrete and how bacteria with cellulose fiber as a carrier serves as a reliable substitute. The increased strength in this creative concrete demonstrates the numerous advantages cellulose fibers provide and highlights its potential for resilient and sustainable building methods.

3.6. Effect of Temperature on Concrete Strength

When comparing the control concrete (CCxx) with the FBCxx concrete, the results from Fig. 7c&d shows that the compressive strength of CCxx decreases by 45.8 %, 56.5 %, 74 %, and 80.5 % within 30–150 min of oven heating, respectively. After the annealing

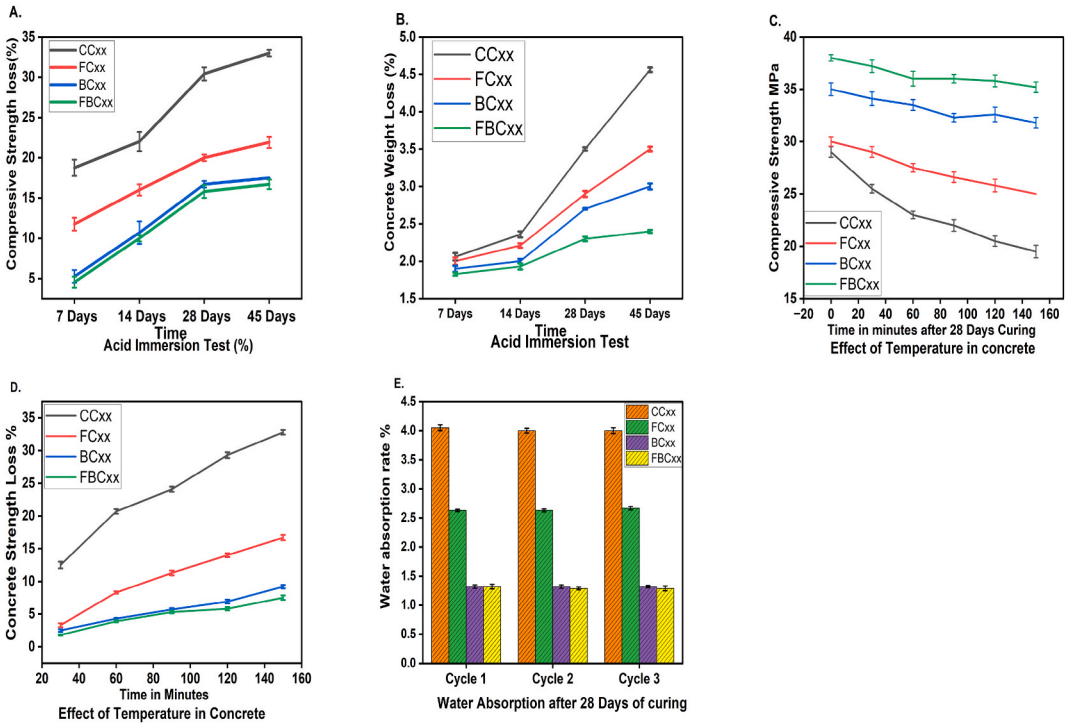

Fig. 7. Effect of acid immersion and high temperature on concrete strength, and water absorption of concrete. (a) acid immersion on concrete compressive strength, (b) % of concrete weight loss due to acid immersion, (c) compressive strength of concrete after oven heating at 426 °C, (d) concrete strength loss %, after oven heating, and (e) concrete water absorption rate after 28 days of curing.

at high temperature, CCxx (control concrete) loses 30–45 % of its original strength. This results from the degradation in bonding between the cement and the aggregates in the concrete with a rise in temperature. Adding cellulose fiber and *LSB* during the mixing process is recommended to minimize the loss of concrete strength at high temperatures. Cellulose fibers provide insulation and stability by acting as a protective shield around the bacteria.

3.7. Water absorption of concrete

After 28 days of curing, the mean water absorption of CCxx, FCxx, BCxx, and FBCxx concrete is 4 %, 2.64 %, 1.32 %, and 1.30 %, respectively, according to the results from Fig. 7e. The water absorption of the concrete was found to decrease from 4 % to 2.64 % with the addition of 0.45 % cellulose fiber and to 1.32 % with the addition of bacteria alone. The water was further decreased to 1.30 % when bacteria were transported by cellulose-based fibers (FBCxx), suggesting a decrease of roughly 67.5 % compared to the control concrete from CCxx.

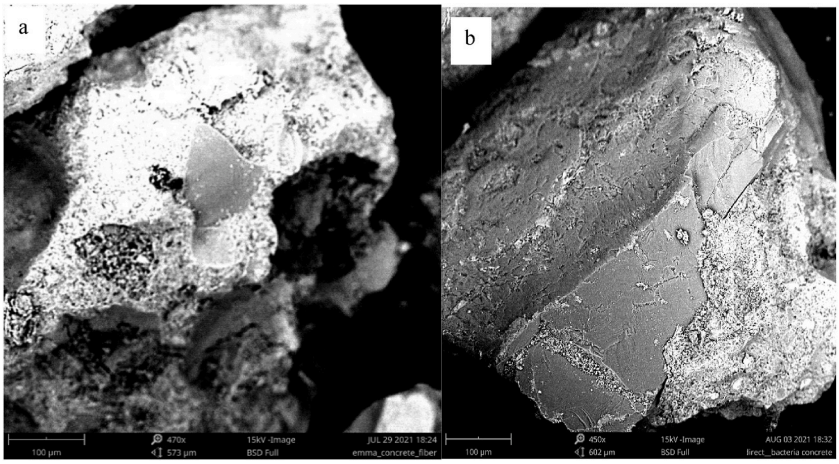

Fig. 8. SEM observations of closely packed calcite particles after self-healing of (a) FBCxx concrete and (b) BCxx concrete.

3.8. Microstructure characterization and crystal formation

Fig. 8 displays the results of the SEM examination of the concrete from BCxx and FBCxx, which shows that self-healing has occurred because of the calcium carbonate release in the cracking area. The images show the formation of tightly packed calcium carbonate due to continuous water retention. After 30 days, the concrete had an elevated pH level and an elevated level of precipitation of calcium carbonate over the fractures, owing to self-healing in both wet-dry and fully wet conditions.

In the X-ray investigation, we observed the first peak in Fig. 9, which indicates the presence of calcium carbonate at an angle of $2\theta = 21^{\circ}$. The peaks observed in earlier research [19,20] are in accordance with this peak. We used the High Score Plus software to determine the crystalline structure of the peak pattern. The X-ray diffractogram shows that both quartz (SiO_2) and calcite ($CaCO_3$) are visible throughout the spectrum. The test results confirm self-healing of the cracks.

3.9. Self-healing of concrete consisting of bacteria

In addition to Figs. 9 and 10 suggests that incorporating bacteria in BCxx and utilizing cellulose fiber as a carrier for bacteria in FBCxx concrete proved successful in restoring concrete fractures within the crack width range from 1.5 mm to 2.5 mm. It is noted that the crack width healed in this study doubles and triples the crack width studied previously [30,31]. This healing was achieved through the wet-dry and fully wet methods after a healing period of 30 days. Notably, by the 30th day, a comprehensive healing of the cracks was observed, accompanied by the precipitation of calcium carbonate. The outcomes highlight how effective bacterial inclusion is at promoting significant self-healing of concrete fractures, especially when the bacteria are carried by cellulose fiber. The capacity for total healing and the calcium carbonate formation that was seen demonstrate the exciting possibilities of adding novel materials, like cellulose fibers, for improved concrete durability and restorative properties. The chemical reaction during the bacteria-induced calcification can be represented by **Equations (1)–(7)** [20]:

$$Ca\,(NH_2)_2 + H_2O = NH_2COOH + NH_3 \quad (1)$$

$$NH_2\,COOH + H_2O = NH_3 + H_2CO_3 \quad (2)$$

$$H_2CO_3 = HCO_3^- + H^+ \quad (3)$$

$$2NH_3 + 2H_2O = 2NH_4^+ + 2OH^- \quad (4)$$

$$HCO_3^- + H^+ 2NH_4^+ + 2OH^- = CO_3^{2-} + 2NH_4^+ + 2H_2O \quad (5)$$

$$Ca^{2+} + Cell = Cell - Ca^{2+} \quad (6)$$

$$Cell - Ca^{2+} + CO_3^{2-} = CaCO_3 - Cell \quad (7)$$

The information about the split tensile and compression strengths of the healed concrete is given in Tables 3 and 4. Per the tables, the self-healed concrete has recovered between 65 % and 70 % of its initial compressive and tensile strength before experiencing any damage. Notably, the control concrete (CCxx) has a lower compressive strength than the samples from FBCxx and BCxx, even after they have been damaged and healed. This suggests the effective restoration of both compressive and tensile strength following self-healing. An intriguing observation is the consistent increase in strength over time during the healing process. This leads to considering conducting future research to determine the specific duration required for the concrete to reach 100 % strength. These findings highlight the intriguing possibility of incorporating bacteria into cellulose fibers for self-healing applications, demonstrating a significant strength recovery and the capacity to outperform the initial strength of traditional concrete.

4. Conclusions

This research presents a pioneering methodology for the autonomous healing of macroscopic cracks in concrete, facilitated by *encapsulating Lysinibaccilus Sphaericus Bacteria (LSB)* within cellulose fibers. This approach, significantly augmented using a 3D-printed polymeric scaffold for preliminary observations, has demonstrated a notable enhancement in concrete mechanical properties. The experimental findings indicated that integrating *LSB*-encapsulated by cellulose fibers into concrete resulted in a substantial 25 % increase in split tensile and compressive strength compared to control samples. Actually, after crack healing, the FBCxx and BCxx still have higher split tensile and compressive strength than those of the control concrete without damage. Additionally, the self-healing capability of this composite material was convincingly evidenced through the closure of cracks up to 2.5 mm in fully wet environments and 1.5 mm in wet-dry conditions within 30 days. The crack width healed in this study doubled or even tripled that achieved in previous studies using cellulose fiber carried bacteria. The test results validate that self-healing of concrete by cellulose fiber carried bacteria is a new alternative for sustainable concrete constructions.

CRediT authorship contribution statement

Emmanuel Igbokwe: Writing – original draft, Visualization, Validation, Methodology, Investigation, Formal analysis, Data curation, Conceptualization. **Samuel Ibekwe:** Project administration, Funding acquisition. **Patrick Mensah:** Supervision, Resources, Funding acquisition. **Ogad Agu:** Investigation, Data curation. **Guoqiang Li:** Writing – review & editing, Resources, Methodology,

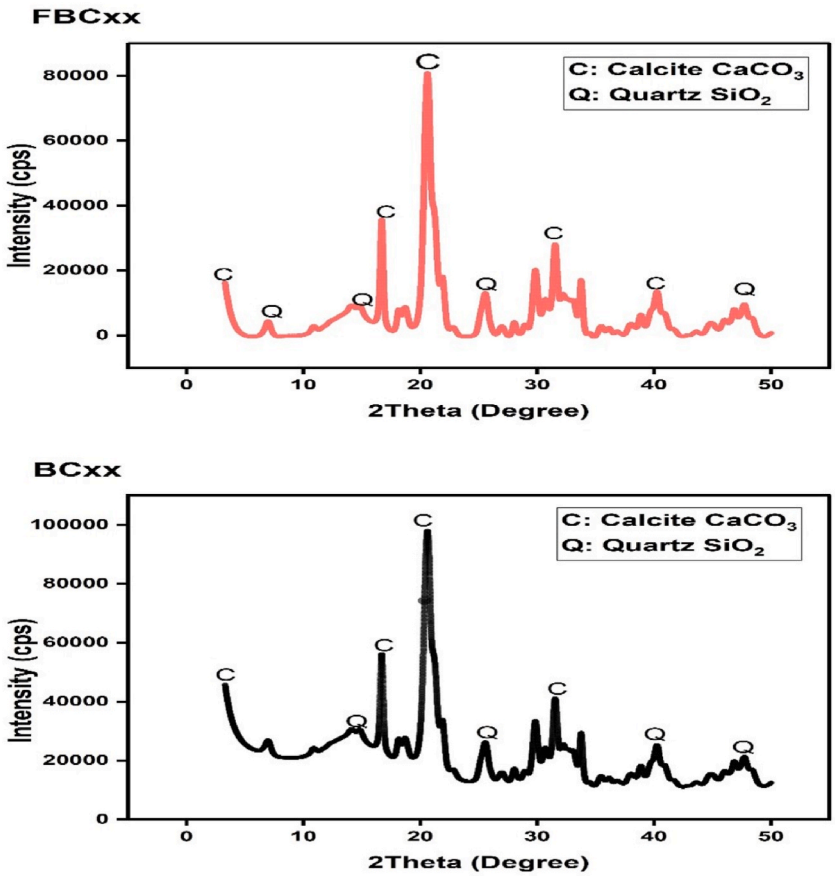

Fig. 9. X-ray diffraction of crystal formation of FBCxx and BCxx concrete.

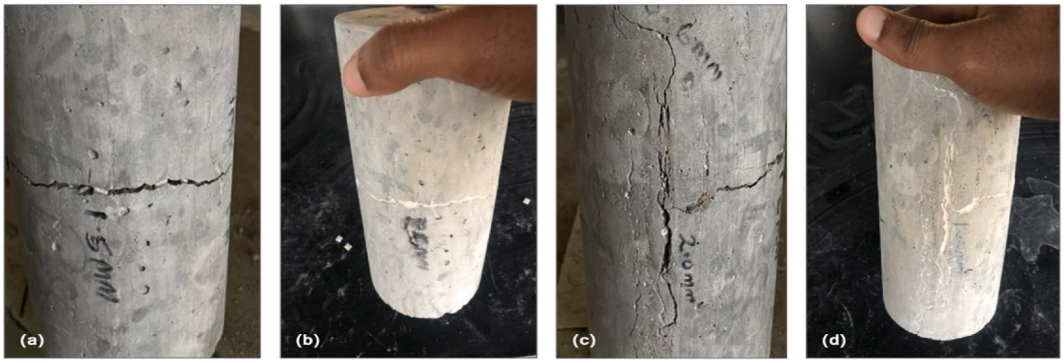

Fig. 10. Visualization of self-healing of the concrete. (a&b) BCxx concrete under wet-dry conditions, and (c&d) FBCxx concrete under fully wet conditions after 30 days of healing.

Table 3
Concrete compressive strength before damage and after self-healing.

Specimen	Before Damage (MPa)	After Damage and Self-Healing (MPa)
CCxx (control concrete)	27.0 ± 0.13	–
BCxx (consisting of bacteria directly)	35.0 ± 0.05	27.9 ± 0.22
FBCxx (consisting of bacteria carried by cellulose fibers)	37.0 ± 0.11	32.2 ± 00

Table 4
Concrete split tensile strength before damage and after self-healing.

Specimen	Before Damage (MPa)	After Damage Self-healing (MPa)
CCxx (control concrete)	2.50 ± 0.10	–
BCxx (consisting of bacteria directly)	3.00 ± 00	2.60 ± 0.20
FBCxx (consisting of bacteria carried by cellulose fibers)	3.40 ± 0.01	3.10 ± 0.03

Funding acquisition, Conceptualization.

Declaration of competing interest

The authors declare that they have no known competing financial interests or personal relationships that could have appeared to influence the work reported in this paper.

Data availability

Data will be made available on request.

Acknowledgments

The authors appreciate the National Science Foundation under award number 1736136 and the Department of Mechanical Engineering at Southern University for funding this project. EI, PM, and GL also acknowledge the support by the National Science Foundation under Grant Number OIA-1946231, and the Louisiana Board of Regents for the Louisiana Materials Design Alliance (LAMDA).

Appendix A. Supplementary data

Supplementary data to this article can be found online at https://doi.org/10.1016/j.jobe.2024.109383.

References

[1] S.A. Puranik, S. Jain, G. Sritam, S. Sandbhor, Bacterial Concrete- a sustainable solution for concrete maintenance, Int. J. Innovative Technol. Explor. Eng. 8 (11S) (2019) 227–232, https://doi.org/10.35940/ijitee.k1046.09811s19.
[2] S. Ganesh, Experimental study on self-healing concrete with the effect of Bacillus subtilis bacteria to improve the strength and sustainability of concrete, Journal of Green Engineering 10 (4) (2020) 1909–1923. https://www.researchgate.net/publication/341804025_Experimental_Study_on_Self-healing_Concrete_with_the_Effect_of_Bacillus_Subtilis_Bacteria_to_Improve_the_Strength_and_Sustainability_of_the_Concrete.
[3] American Society of Civil Engineers News Release, Publ. Works Manag. Pol. 4 (1) (1999) 58–80, https://doi.org/10.1177/1087724x9941007.
[4] G. Li, S. Pang, J.E. Helms, D. Mukai, S. Ibekwe, W. Alaywan, Stiffness degradation of FRP strengthened RC beams subjected to hygrothermal and aging attacks, J. Compos. Mater. 36 (7) (2002) 795–812, https://doi.org/10.1177/0021998302036007614.
[5] G. Li, S. Hedlund, S. Pang, W. Alaywan, J. Eggers, C. Abadie, Repair of damaged RC columns using fast curing FRP composites, Compos. B Eng. 34 (3) (2003) 261–271, https://doi.org/10.1016/s1359-8368(02)00101-4.
[6] X. Ma, L. Liu, Fatigue properties of RC beams reinforced with ECC layer and steel plate, Construct. Build. Mater. 372 (2023) 130799, https://doi.org/10.1016/j.conbuildmat.2023.130799.
[7] K. Van Tittelboom, N. De Belie, Self-healing in cementitious materials—a review, Materials 6 (6) (2013) 2182–2217, https://doi.org/10.3390/ma6062182.
[8] L.R. De Souza, A. Al-Tabbaa, Microfluidic fabrication of microcapsules tailored for self-healing in cementitious materials, Construct. Build. Mater. 184 (2018) 713–722, https://doi.org/10.1016/j.conbuildmat.2018.07.005.
[9] S.R. White, N.R. Sottos, P.H. Geubelle, J.S. Moore, M.R. Kessler, S.R. Sriram, E.N. Brown, S. Viswanathan, Autonomic healing of polymer composites, Nature 409 (2001) 794–797, https://doi.org/10.1038/35057232.
[10] J.Y. Wang, N. De Belie, W. Verstraete, Diatomaceous earth as a protective vehicle for bacteria applied for self-healing concrete, J. Ind. Microbiol. Biotechnol. 39 (4) (2012) 567–577, https://doi.org/10.1007/s10295-011-1037-1.
[11] J. Wang, D. Snoeck, S. Van Vlierberghe, W. Verstraete, N. De Belie, Application of hydrogel encapsulated carbonate precipitating bacteria for approaching a realistic self-healing in concrete, Construct. Build. Mater. 68 (2014) 110–119, https://doi.org/10.1016/j.conbuildmat.2014.06.018.
[12] J. Wang, H. Soens, W. Verstraete, N. De Belie, Self-healing concrete by use of microencapsulated bacterial spores, Cement Concr. Res. 56 (2014) 139–152, https://doi.org/10.1016/j.cemconres.2013.11.009.
[13] A.C. Ganesh, M. Muthukannan, R. Malathy, C.R. Babu, An experimental study on effects of bacterial strain combination in fiber concrete and Self-Healing efficiency, KSCE J. Civ. Eng. 23 (10) (2019) 4368–4377, https://doi.org/10.1007/s12205-019-1661-2.
[14] A. Xin, Y. Su, S. Feng, M. Yan, K. Yu, Z. Feng, K.H. Lee, L. Sun, Q. Wang, Growing living composites with ordered microstructures and exceptional mechanical properties, Adv. Mater. 33 (13) (2021) 2006946, https://doi.org/10.1002/adma.202006946.
[15] H. Jonkers, A.P. Thijssen, G. Muyzer, O. Çopuroğlu, E. Schlangen, Application of bacteria as self-healing agent for the development of sustainable concrete, Ecol. Eng. 36 (2) (2010) 230–235, https://doi.org/10.1016/j.ecoleng.2008.12.036.
[16] P.Q. Nguyen, N.D. Courchesne, A. Duraj-Thatte, P. Praveschotinunt, N. Joshi, Engineered Living Materials: prospects and challenges for using biological systems to direct the assembly of smart materials, Adv. Mater. 30 (19) (2018) e1704847, https://doi.org/10.1002/adma.201704847.
[17] S. Luhar, S. Gourav, A review paper on self-healing Concrete, J. Civ. Eng. Res. 5 (3) (2015) 53–58. http://www.sapub.org/global/showpaperpdf.aspx?doi=10.5923/j.jce.20150503.01.
[18] H. Huang, G. Ye, A review on self-healing in reinforced concrete structures in view of serving conditions, in: 3rd International Conference on Service Life Design for Infrastructure, 2014, pp. 375–388. *Zhuhai, China*, http://resolver.tudelft.nl/uuid:bc600001-17ed-4a9b-8e47-b54226e17903.
[19] H. Huang, G. Ye, C. Qian, E. Schlangen, Self-healing in cementitious materials: materials, methods, and service conditions, Mater. Des. 92 (2016) 499–511, https://doi.org/10.1016/j.matdes.2015.12.091.

[20] J. Dick, W. De Windt, B. De Graef, H. Saveyn, P. Van Der Meeren, N. De Belie, W. Verstraete, Bio-deposition of a calcium carbonate layer on degraded limestone by Bacillus species, Biodegradation 17 (4) (2006) 357–367, https://doi.org/10.1007/s10532-005-9006-x.
[21] G. Li, D. Nettles, Thermomechanical characterization of a shape memory polymer based self-repairing syntactic foam, Polymer 51 (3) (2010) 755–762, https://doi.org/10.1016/j.polymer.2009.12.002.
[22] G. Li, N. Uppu, Shape memory polymer based self-healing syntactic foam: 3-D confined thermomechanical characterization, Compos. Sci. Technol. 70 (9) (2010) 1419–1427, https://doi.org/10.1016/j.compscitech.2010.04.026.
[23] M.A. Meyers, P. Chen, M. López, Y. Seki, A.Y. Lin, Biological materials: a materials science approach, J. Mech. Behav. Biomed. Mater. 4 (5) (2011) 626–657, https://doi.org/10.1016/j.jmbbm.2010.08.005.
[24] A.Y. Chen, C. Zhong, T.K. Lu, Engineering living Functional materials, ACS Synth. Biol. 4 (1) (2015) 8–11, https://doi.org/10.1021/sb500113b.
[25] U.G.K. Wegst, H. Bai, E. Saiz, A.P. Tomsia, R.O. Ritchie, Bioinspired structural materials, Nat. Mater. 14 (1) (2014) 23–36, https://doi.org/10.1038/nmat4089.
[26] H. Smith, A. Brown, Benson's Microbiological Applications Laboratory Manual. ISBN10: 126025898X, McGraw Hill, 2016. https://www.mheducation.com/highered/product/benson-s-microbiological-applications-laboratory-manual-brown-smith/M9781260258981.html.
[27] Y. Yan, G. Jia, Y. Zhang, Y. Gao, Z. Li, The influence of expanded perlite as a bio-carrier on the freeze–thaw properties of self-healing concrete, Construct. Build. Mater. 409 (2023) 133891, https://doi.org/10.1016/j.conbuildmat.2023.133891.
[28] P. Risdanareni, J. Wang, N. Boon, N. De Belie, Alkali activated lightweight aggregate as bacterial carrier in manufacturing self-healing mortar, Construct. Build. Mater. 368 (2023) 130375, https://doi.org/10.1016/j.conbuildmat.2023.130375.
[29] Y. Su, C. Qian, Y. Rui, J. Feng, Exploring the coupled mechanism of fibers and bacteria on self-healing concrete from bacterial extracellular polymeric substances (EPS), Cement Concr. Compos. 116 (2021) 103896, https://doi.org/10.1016/j.cemconcomp.2020.103896.
[30] H. Singh, R. Gupta, Influence of cellulose fiber addition on self-healing and water permeability of concrete, Case Stud. Constr. Mater. 12 (2020) e00324, https://doi.org/10.1016/j.cscm.2019.e00324.
[31] H. Singh, R. Gupta, Cellulose fiber as bacteria-carrier in mortar: self-healing quantification using UPV, J. Build. Eng. 28 (2020) 101090, https://doi.org/10.1016/j.jobe.2019.101090.
[32] ASTM C150/C150M - 20, Standard Specification for Portland Cement https://www.astm.org/standards/c150.
[33] UltraFiber 500 documentation | Solomon Colors. (n.d.).https://www.solomoncolors.com/pages/ultrafiber/documentation-uf500.php#gsc.tab=0.